The Many Faces of Granulomatosis With Polyangiitis: A Review of the Head and Neck Imaging Manifestations

Marius G. Pakalniskis[1]
Aaron D. Berg[1]
Bruno A. Policeni[1]
Lindell R. Gentry[2]
Yutaka Sato[1]
Toshio Moritani[1]
Wendy R. K. Smoker[1]

OBJECTIVE. Wegener granulomatosis has recently been renamed as granulomatosis with polyangiitis (GPA). In this review, we examine the clinical criteria and pathologic and pathophysiologic mechanisms of GPA, with an emphasis on findings encountered in the realm of head and neck imaging. Particular attention is paid to generating an appropriate differential diagnosis, because many of the imaging features of GPA overlap with those of other diseases, most notably lymphoma and sarcoidosis. Recent therapeutic advancements have underscored the importance of the radiologist in suggesting the diagnosis early, resulting in earlier treatment and decreased patient morbidity. This is particularly true for the head and neck manifestations of GPA; although they are less common, they often herald a refractory disease course that requires aggressive immunosuppressive therapy. Knowledge of common and uncommon imaging findings enables the radiologist to diagnose GPA early enough to start treatment promptly and reduce patient morbidity.

CONCLUSION. Although there are no reliable pathognomonic imaging features for GPA, the present article attempts to identify patterns of disease that are suggestive of the disease. The diagnosis ultimately relies on a constellation of radiographic findings, laboratory values, and accurate clinical history.

Dr. Friedrich Wegener wrote two articles in the late 1930s, both describing a syndrome characterized by chronic rhinitis and renal failure with histologic features of granulomatous necrotizing inflammation [1, 2]. The syndrome bore his name for decades. Although the eponymic term referenced a controversial historical physician with Nazi party ties, the new name, granulomatosis with polyangiitis (GPA), reflects the pathologic basis of the disease.

The prevalence of GPA in the United States is estimated to be three cases per 100,000 population with a male-to-female ratio of 1:1. The disease may present at any age but is more common in the fourth and fifth decades. Most (73–99%) of the 2300 new annual diagnoses of GPA in the United States will involve the head and neck, and a substantial number (10–45% of cases) will affect the CNS [3, 4]. GPA-related CNS disease has become a recent focus of clinical attention because of its high association with a refractory disease course [3].

Diagnostic challenges stem from the varied manifestations of GPA, with its ability to affect almost any organ system, including the CNS. Hence, a standardized clinical diagnostic framework has yet to be established. Laboratory values, such as elevated antineutrophil cytoplasmic antibodies (ANCA) are important; however, a quarter of patients with limited GPA have no detectable ANCA, further confounding the diagnostic dilemma.

Since Dr. Wegener's seminal articles were published nearly 80 years ago, numerous additional manifestations of GPA have been unveiled in step with an immunologically based understanding of the disease. ANCAs produced by B lymphocytes are thought to be the pathogenic crux. The pathogenic role of B lymphocytes explains the therapeutic success of rituximab in controlling disease activity on the basis of its selective targeting of these cells [5]. The efficacy of cyclophosphamide has also been largely explained by its cytotoxic effect on B lymphocytes [5].

ANCAs primarily target an enzyme expressed at the surface of neutrophils, proteinase-3, whose subsequent activation initiates a transduction cascade that both enhances neutrophil adhesion to endothelium and promotes the release of lytic enzymes

Keywords: CNS, granulomatosis with polyangiitis, head and neck, neuroradiology, orbit, sinonasal, Wegener granulomatosis

DOI:10.2214/AJR.14.13864

Received September 11, 2014; accepted after revision May 6, 2015.

[1]Department of Radiology, University of Iowa Hospitals and Clinics, 200 Hawkins Dr, Iowa City, IA 52246. Address correspondence to M. G. Pakalniskis (mgpaka@uw.edu).

[2]Department of Radiology, University of Wisconsin Hospitals and Clinics, Madison, WI.

WEB
This is a web exclusive article.

AJR 2015; 205:W619–W629

0361–803X/15/2056–W619

[5]. The resulting pathologic manifestation is characterized by necrotizing granulomas, tissue necrosis, and variable amounts of vasculitis in small-to-medium vessels. The cause of B-lymphocyte production of ANCA is poorly understood; however, a combination of predisposing genetic factors and environmental triggers, most notably *Staphylococcus aureus*, is among the leading theories [6].

TABLE 1: Differential Diagnoses for Granulomatosis With Polyangiitis (GPA)–Related Sinonasal Disease

Diagnosis	Symptoms					
	Hard-Palate Defect	Mucosal Nodularity	Septal Destruction	Erosions	Neoosteogenesis	Soft-Tissue Mass
GPA		Present	Present	Present	Present	
Nasal cocaine necrosis	Present		Present	Present		
Sarcoidosis		Present		Present	Present	
Lymphoma	Present		Present	Present		Present

Pathologic Profile

GPA characteristically presents with nasal involvement accompanied by pulmonary and renal disease. Histopathologic analysis of nasal tissue reveals a leukocytoclastic vasculitis with geographic necrosis surrounded by palisaded histiocytes [7]. The constellation of vasculitis, necrosis, and granulomatous inflammation, however, is seen in only 16% of nasal biopsy specimens [8]. When dense lymphocytic infiltrate is encountered, malignant lymphoma is an important diagnostic alternative, because GPA is not a lymphocyte-rich process.

The predominant gross pathologic change in the lungs is liquefactive or coagulative necrosis, with microscopy revealing necrotizing granulomas that are generally not as clearly demarcated as those seen in tuberculosis or sarcoidosis [9] (Fig. 1). Angiitis is a requisite for diagnosis. The most common renal lesion is a focal necrotizing glomerulonephritis, often showing crescents. Renal papillary necrosis is a complication in up to 20% of patients with GPA [10]. Necrotizing vasculitis is less commonly observed in kidney biopsies.

Two distinct forms of GPA exist: limited and severe. Limited GPA was traditionally defined as being isolated to the respiratory tract and sparing the kidneys; however, the definition has recently been revised to include manifestations of GPA that pose no immediate threat to life or vital organ function. The severe form, in contrast, does pose such a threat [11]. The distinction has important therapeutic implications because patients with limited GPA typically respond favorably to less-toxic regimens of methotrexate and glucocorticoids, whereas severe GPA often requires aggressive therapy with glucocorticoids and the addition of cyclophosphamide [11].

CNS involvement shows three identifiable pathologic patterns of disease: first, vasculitis affecting small-to-medium vessels of the brain or spinal cord; second, granulomatous masses originating from the sinonasal or orbital compartments and perforating through adjacent bone to invade the meninges and the brain; and third, granulomatous lesions developing de novo within intracranial tissue, such as the meninges or the brain [12].

Sinonasal Involvement in Granulomatosis With Polyangiitis

The imaging features of granulomatous involvement of the sinonasal compartment include osseous erosion and destruction, mucosal thickening, and neoosteogenesis. Osseous erosion has a predilection for the anterior ethmoid region; however, sites of erosion involving the posterior ethmoid, sphenoid, and frontal and maxillary sinuses have also been described [12]. CT best reveals the erosive changes characterized by punctate osseous destruction.

Mucosal thickening most frequently affects the maxillary sinus [13]. Although it is similar in appearance to chronic sinusitis, a pattern of nodular thickening may suggest GPA [14].

Obliterative osseous changes, which affect up to 75% of patients with GPA, have a distribution that is unique from that of erosions. The destructive process is initially localized to the midline septum and turbinates and spreads symmetrically to the adjacent antra and, eventually, the remainder of the sinuses, resulting in a large single sinus cavity (Fig. 2). The hard palate is characteristically spared [15]. Avascular necrosis is thought to underpin the pathophysiologic process of bony destruction caused by an inflammatory cell infiltrate occluding small arteries [15, 16].

The combination of osseous destruction and neoosteogenesis further narrows the differential diagnosis in favor of GPA. These changes are most commonly seen in the antra [15]. The process of neoosteogenesis is seen in up to 50% of patients with GPA, and CT may reveal a distinctive sclerotic appearance: a leading edge of well-corticated bone paralleling the sinus wall and overlying an area of less-dense bone [15] (Fig. 3). The less-dense bone may show high signal on T1-weighted MRI sequences, suggesting marrow deposition and favoring a process of neoosteogenesis rather than periostitis.

The imaging features of GPA-induced sinonasal disease overlap with those of several aforementioned entities that together form a differential diagnosis, most notably nasal cocaine necrosis, sarcoidosis, and extranodal nasal lymphoma (Table 1). A clinical history of cocaine use will often clinch the diagnosis of nasal cocaine necrosis. Hard palate defects are common with nasal cocaine necrosis and lymphoma [17], whereas they are distinctly uncharacteristic of GPA. Osseous erosion underlying mucosal inflammation is not pathognomonic for GPA and can be seen in both sarcoidosis and T-cell lymphoma [12]. However, erosions affecting the nasal septum and turbinates may be more specific for GPA [18]. Lymphoma will often present with a large midline soft-tissue mass, which is not characteristic of GPA. Sarcoidosis can be indistinguishable from GPA on imaging; however, frank nasal septal destruction is not a characteristic feature of sarcoidosis [19].

Airway Involvement in Granulomatosis With Polyangiitis

Airway involvement is found in up to 55% of patients with GPA, typically occurring as a late complication with disease manifestations seen elsewhere in the body [20]. On the rare occasion when there is isolated involvement of the respiratory tract, about 20% of patients will have undetectable ANCA levels, which presents a significant diagnostic challenge. Moreover, the radiographic features of laryngeal and endobronchial involvement are nonspecific, revealing inflammatory changes of circumferential mucosal thickening, irregularity, and ulceration that are best appreciated on CT [21]. A high clinical suspicion, therefore, is necessary for the correct diagnosis of GPA limited to the respiratory tract.

Long-term mucosal inflammation with subsequent fibrosis eventually causes sub-

TABLE 2: Differential Diagnoses for Airway Involvement in Granulomatosis With Polyangiitis (GPA)

Diagnosis	Symptoms					
	Cavitary Lung Nodules	Circumferential Mucosal Thickening	Subglottic Stenosis	Airway Mass	Calcification	Adenopathy
GPA	Present	Present	Present	Present		
Postintubation		Present	Present			
Tracheal neoplasm			Present	Present		Present
Amyloidosis		Present	Present	Present	Present	
Relapsing polychondritis			Present			
Sarcoidosis		Present	Present			Present

glottic stenosis, the most common airway manifestation in GPA [22]. Stenosis caused by chronic fibrotic scarring is refractory to systemic immunosuppressive therapy [23]. Most tracheal stenoses are caused by prolonged tracheal intubation [24]; however, the presence of peristenotic mucosal thickening and coexistent pulmonary nodules and cavitary masses strongly favors GPA. In cases of isolated subglottic stenosis, a clinical history suggestive of GPA, such as epistaxis and uncontrolled sinusitis, becomes integral to the accurate diagnosis.

Airway obstruction can also result from a tracheal or bronchial mass lesion in the form of an inflammatory pseudotumor caused by proliferation of inflammatory tissue, generally during the active stage of GPA [20] (Fig. 4). Tissue diagnosis is often required to exclude malignancy and establish GPA as the cause. Rare cases have been reported of rapid inflammatory tissue growth causing acute airway obstruction and death [25].

The major differential diagnoses for GPA-related airway disease include amyloidosis, tracheal neoplasm, sarcoidosis, relapsing polychondritis, and postintubation tracheal stenosis (Table 2). The presence of concomitant cavitary lung nodules, a finding seen in up to 25% of GPA-induced nodules larger than 2 cm [26], is unique to the diagnosis of GPA. Amyloidosis can present with features similar to those of GPA, including the presence of endotracheal pseudotumor [27]; however, submucosal airway calcifications favors amyloidosis over GPA. A tracheal neoplasm, most commonly squamous cell carcinoma, will typically present as an eccentric mass arising from the tracheal wall, rather than circumferential thickening. The presence of adenopathy, both in the setting of neoplasm and sarcoidosis, is less characteristic of GPA. Relapsing polychondritis characteristically spares the posterior membranous tracheal wall, and postintubation tracheal stenosis will present with a history of intubation.

Orbit Involvement in Granulomatosis With Polyangiitis

Ophthalmologic complications occur in up to 58% of patients with GPA [4]. Orbital imaging will commonly show a diffuse inflammatory infiltrate that molds to the contour of the orbit with occasional extension into the adjacent sinuses [28] (Fig. 5). Growth of inflammatory tissue leads to the formation of an orbital pseudotumor, the most common ophthalmologic manifestation of GPA [29] (Fig. 6). The resulting proptosis is a helpful clinical sign when airway disease or glomerulonephritis are simultaneously observed. Similar to the aforementioned cases of GPA limited to the respiratory tract, ANCA titers may be negative when ocular disease is the only manifestation in up to 10% of patients with GPA [4, 29].

Most orbital pseudotumors are unilateral and either extraconal or transspatial (both extra- and intraconal) in distribution. Only about 5% of masses are isolated to the intraconal compartment. Complications include optic nerve compression with subsequent atrophy and visual loss [29, 30]. Extension of the granulomatous pseudotumor to involve the cranial nerves of the intracavernous sinus may be manifest as Tolosa-Hunt syndrome, which is characterized by recurrent painful ophthalmoplegia [31].

Orbital socket contracture is an additional complication that occurs during the late stage of orbital pseudotumor formation. Imaging reveals enophthalmos and infiltration of the orbit with fibrotic tissue, showing characteristic low T1 and high T2 signals on MRI [32]. Fibrosis retracts the optic globe, resulting in chronic orbital pain, ischemic optic neuritis, and subsequent blindness [29]. Approximately one third of patients with GPA with chronic orbital disease develop orbital contraction. Immunosuppressive therapy may be responsible for inciting contracture development. The fibrotic nature of the contraction makes it refractory to treatment [32].

Several entities may present with imaging findings that resemble those of GPA-related orbital disease, including sarcoidosis, lymphoma, cellulitis, cavernous hemangioma, and venolymphatic malformations (Table 3). Orbital sarcoid reaction is the term used to describe sarcoidosis presenting as

TABLE 3: Differential Diagnoses for Granulomatosis With Polyangiitis (GPA)–Related Orbital Disease

Diagnosis	Symptom					
	Orbital Mass	Lacrimal Gland Infiltration	Bone Destruction	Subperiosteal Abscess	Calcification	Fluid Levels
GPA	Present		Present			
Lymphoma	Present	Present				
Sarcoidosis	Present	Present	Present			
Cellulitis				Present		
Cavernous hemangioma	Present				Present	
Venolymphatic malformation	Present					Present

a disease limited to the orbit without systemic involvement. An enhancing intraorbital pseudotumor can form in patients with sarcoidosis and therefore mimic GPA; however, sarcoidosis characteristically causes concomitant granulomatous lacrimal gland infiltration [33], presenting as enlarged and diffusely enhancing bilateral lacrimal glands, which are an uncommon feature of GPA. Lymphoproliferative lesions of the orbit, most commonly B-cell lymphoma, also have a predilection for involving the lacrimal glands as well as the anterior extraconal space [34]. Furthermore, bone destruction is not a characteristic feature of lymphoma [35], unlike GPA, wherein sinonasal destruction may be seen concurrently with an orbital pseudotumor. Intraorbital postseptal cellulitis does not typically present as a discrete orbital mass. Clinical symptoms of fever and orbital swelling, as well as the formation of a subperiosteal abscess in the medial extraconal orbit, would support the diagnosis of cellulitis. A cavernous hemangioma will present as a well-encapsulated orbital mass, most commonly in the intraconal compartment, whereas a GPA pseudotumor rarely presents within this compartment. Cavernous hemangiomas also occasionally calcify [36], in contradistinction to GPA pseudotumors. Venolymphatic malformations are transspatial orbital masses with characteristic fluid-fluid levels on T2-weighted images that are not observed in GPA [36].

Skull Base Involvement in Granulomatosis With Polyangiitis

Skull base involvement in GPA commonly results from direct extension of the neighboring granulomatous sinonasal or orbital lesion. A resulting cranial neuropathy occurs in approximately 6% of patients [37]. MRI will reveal inflammatory changes with associated thickening and enhancement of the adjacent cranial nerves (Fig. 7). When multiple cranial neuropathies are observed simultaneously, the distribution is predominantly unilateral [37]. The olfactory nerve (cranial nerve I) and optic nerve (cranial nerve II) are involved with greatest frequency, although nearly every cranial nerve is vulnerable [29, 37]. Olfactory dysfunction has recently been recognized as a relatively common finding in patients with GPA; however, the extent to which it is related to inflammation or therapy is unknown [38].

The optic nerve is most commonly involved by being compressed by an adjacent orbital granuloma, leading to nerve atrophy. Less commonly, vasculitis of the posterior ciliary arteries or the central retinal artery may cause ischemic optic neuropathy or retinal ischemia, respectively [39], and blindness may result. Optic neuritis is among the rarest of GPA-related optic nerve diseases [40]. On T2-weighted MRI, acute optic neuritis will manifest as a hyperintense signal in an enlarged enhancing optic nerve.

The differential diagnosis for cranial neuropathies mimicking GPA includes multiple sclerosis, sarcoidosis, lymphoma, and perineural tumor spread. GPA-related optic neuritis may be confused for the presenting sign of multiple sclerosis. The presence of periventricular T2-hyperintense white matter lesions would favor the diagnosis of multiple sclerosis. As previously mentioned, sarcoidosis and lymphoma are mimickers of GPA and can manifest as enlarged enhancing cranial nerves; however, sarcoidosis more commonly presents in a bilateral distribution [41], and lymphoma (both primary and secondary) will typically show brain parenchymal involvement [42]. Perineural tumor spread from head and neck cancers most commonly affects cranial nerves V and VII, whereas cranial nerves I and II are most frequently involved in GPA. Moreover, skull base foraminal enlargement is characteristic of perineural extension of malignancy and is not a feature of GPA.

Temporal Bone Involvement in Granulomatosis With Polyangiitis

Otologic manifestations occur in up to 40% of patients with GPA [43, 44]. Direct extension of adjacent sinonasal disease is responsible for obstructing the eustachian tube and ultimately

TABLE 4: Differential Diagnoses for Intracranial Manifestations of Granulomatosis With Polyangiitis (GPA)

	Symptom								
Area of CNS, Diagnosis	Enhancement	Patchy High T2 Signal	DWI Restriction	U-Fiber Involvement	Enlargement	Meningeal Enhancement	Pial Involvement	Fever	Dural Mass
Brain parenchyma									
GPA	Present	Present	Present						
PML		Present		Present					
Acute disseminated encephalomyelitis	Present	Present		Present					
Pituitary gland									
GPA					Present				
Lymphoma					Present				
Sarcoidosis					Present				
LCH					Present				
Metastasis					Present				
Dura									
GPA						Present			
Lymphoma						Present			Present
Sarcoidosis						Present	Present		Present
Infection						Present		Present	

Note—PML = progressive multifocal leukoencephalopathy, LCH = Langerhans cell histiocytosis.

causing a serous otitis media, the most common otologic finding [45]. Conductive hearing loss of the affected side is a common clinical manifestation. Bilateral otitis media in an adult patient should alert the clinician to the possibility of GPA. CT may show opacification of the bilateral middle ears and mastoid air cells with thickening of the bony septa.

The differential diagnosis for temporal bone involvement includes coalescent otomastoiditis and osteoradionecrosis. Granulomatous inflammation can cause bone destruction that mimics coalescent otomastoiditis [46]; however, the presence of associated complications, such as epidural abscess or sinus thrombosis, would favor an infectious cause. Furthermore, coalescent otomastoiditis tends to be a unilateral disease much like osteoradionecrosis, another differential consideration that presents as moth-eaten bony destruction within the distribution of a known radiation port, typically in patients with head and neck cancer.

Intracranial Involvement in Granulomatosis With Polyangiitis

GPA manifests within the intracranial compartment by involving the brain parenchyma, pituitary gland, and dura. Cerebral small-vessel vasculitis occurs in approximately 4% of patients with GPA and is the most common parenchymal manifestation. It has been associated with seizures, intracranial hemorrhage, transient ischemic attacks, and arterial or venous thrombosis [37]. Imaging of GPA-induced cerebral vasculitis reveals white matter lesions with patchy high T2 signal intensity in a typical vascular distribution [47]. DWI can show areas of infarction, and contrast-enhanced images may show patchy regions of enhancement (Fig. 8).

The differential diagnosis for parenchymal disease (Table 4) includes CNS infection, most notably progressive multifocal leukoencephalopathy (PML) and acute disseminated encephalomyelitis. PML is an important differential diagnosis to consider in patients with GPA undergoing immunosuppressive therapy [48]. The characteristic subcortical U-fiber involvement encountered in PML, as well as the absence of diffusion restriction and parenchymal enhancement, will favor PML. Acute disseminated encephalomyelitis can have a similar imaging appearance but will usually be preceded by either a vaccination or an upper respiratory infection.

Involvement of the pituitary gland will typically present with posterior lobe insufficiency in the form of central diabetes insipidus. The most common imaging feature is an enlarged pituitary gland [49]. The enlarged gland may cause compression of the pituitary stalk with resultant hyperprolactinemia [29]. The pathophysiologic process of pituitary involvement includes direct extension of adjacent sinonasal disease, in situ granuloma formation, and vasculitis of the pituitary blood vessels [49].

MRI of the pituitary gland reveals an enlarged gland with either heterogeneous or homogeneous enhancement. Cystic changes may also be observed, in addition to increased enhancement and thickening of the infundibulum, especially its superior portion [47, 49]. There is often a loss of the characteristic hyperintense signal in the posterior pituitary on T1-weighted sequences, which is strongly correlated with the clinical manifestation of central diabetes insipidus (Fig. 9). The loss of the posterior pituitary bright spot is thought to result from decreased vasopressin content [50]. Improvement in pituitary function does not always correlate with resolution of imaging abnormalities [49].

No unique imaging characteristics exist that can reliably differentiate GPA from several entities that also cause pituitary enlargement, many of which have been discussed in previous sections. The need to correlate with additional imaging findings and clinical history is especially important when confronted with an enlarged pituitary gland.

Pachymeningitis is the most common form of GPA-related meningeal disease [51]. Most patients present with severe headache refractory to analgesics prompting an MRI examination that reveals linear symmetric thickening and enhancement of dura mater. Meningeal involvement is associated with limited disease [51]. Two distinct patterns of meningeal disease have been recognized. The focal form is contiguous with adjacent sinonasal or orbital disease and represents direct spread of inflammation, whereas diffuse symmetric dural thickening and enhancement is observed independently [47] (Fig. 10).

The differential diagnosis for diffuse symmetric linear meningeal thickening includes lymphoma, neurosarcoid, and infectious meningitis (Table 4). Both lymphoma and neurosarcoid can present with dural masses, which is not a typical feature of GPA. Neurosarcoid has an affinity for involving the pia rather than the dura [52] and will commonly show lacelike leptomeningeal enhancement. Leptomeningitis occurs in only a minority of GPA cases, which further helps distinguish it from infectious meningitis, which is the most emergent differential consideration. A clinical history of fever would support an infectious cause.

Conclusion

The multitude of GPA-induced manifestations presents significant challenges to the diagnostician. This is a relatively rare disease; however, it very commonly involves structures of the head and neck. Although CNS involvement is less common, manifestations are important to recognize because it heralds a refractory disease course requiring more-aggressive immunosuppressive therapy. Immunosuppressive therapy is also not without complications, and these complications can mimic disease progression. By recognizing the common and less-common imaging manifestations, radiologists play a role in both diagnosing GPA and monitoring disease activity. Recognition of active disease can ultimately allow earlier induction of therapy and improved morbidity and mortality. There is no reliable pathognomonic imaging feature that clinches the diagnosis; however, certain patterns of disease are suggestive of GPA. The constellation of radiographic findings, laboratory values, and accurate clinical history is necessary for arriving at the correct diagnosis.

References

1. Wegener F. Ueber eine eigenartige rhinogene Granulomatose mit besonderer Beteiligung des Arteriensystems und der Nieren. *Beitr Pathol Anat* 1939; 102:36
2. Wegener F. Ueber generalisierte septische Gefasserkrankungen. *Verh Deut Pathol Ges* 1936; 29:202–210
3. Holle JU, Gross WL, Holl-Ulrich K, et al. Prospective long-term follow-up of patients with localised Wegener's granulomatosis: does it occur as persistent disease stage? *Ann Rheum Dis* 2010; 69:1934–1939
4. Tarabishy AB, Schulte M, Papaliodis GN, Hoffman GS. Wegener's granulomatosis: clinical manifestations, differential diagnosis, and management of ocular and systemic disease. *Surv Ophthalmol* 2010; 55:429–444
5. Nelson D, Specks U. Granulomatosis with polyangiitis (Wegener's). *Journal* 2011; *Eur Respir Mon* 2011; 54:1–14
6. Stegeman CA, Tervaert JW, Sluiter WJ, Manson WL, de Jong PE, Kallenberg CG. Association of chronic nasal carriage of *Staphylococcus aureus* and higher relapse rates in Wegener granulomatosis. *Ann Intern Med* 1994; 120:12–17

7. Colby TV, Tazelaar HD, Specks U, DeRemee RA. Nasal biopsy in Wegener's granulomatosis. *Hum Pathol* 1991; 22:101–104
8. Devaney KO, Travis WD, Hoffman G, Leavitt R, Lebovics R, Fauci AS. Interpretation of head and neck biopsies in Wegener's granulomatosis: a pathologic study of 126 biopsies in 70 patients. *Am J Surg Pathol* 1990; 14:555–564
9. Heffner DK. Wegener's granulomatosis is not a granulomatous disease. *Ann Diagn Pathol* 2002; 6:329–333
10. Watanabe T, Nagafuchi Y, Yoshikawa Y, Toyoshima H. Renal papillary necrosis associated with Wegener's granulomatosis. *Hum Pathol* 1983; 14:551–557
11. Stone JH; Wegener's Granulomatosis Etanercept Trial Research Group. Limited versus severe Wegener's granulomatosis: baseline data on patients in the Wegener's granulomatosis etanercept trial. *Arthritis Rheum* 2003; 48:2299–2309
12. Grindler D, Cannady S, Batra PS. Computed tomography findings in sinonasal Wegener's granulomatosis. *Am J Rhinol Allergy* 2009; 23:497–501
13. Lohrmann C, Uhl M, Warnatz K, Kotter E, Ghanem N, Langer M. Sinonasal computed tomography in patients with Wegener's granulomatosis. *J Comput Assist Tomogr* 2006; 30:122–125
14. Benoudiba F, Marsot-Dupuch K, Rabia MH, Cabanne J, Bobin S, Lasjaunias P. Sinonasal Wegener's granulomatosis: CT characteristics. *Neuroradiology* 2003; 45:95–99
15. Lloyd G, Lund VJ, Beale T, Howard D. Rhinologic changes in Wegener's granulomatosis. *J Laryngol Otol* 2002; 116:565–569
16. Devaney K, Ferlito A, Hunter BC, Devaney SL, Rinaldo A. Wegener's granulomatosis of the head and neck. *Ann Otol Rhinol Laryngol* 1998; 107:439–445
17. Westreich RW, Lawson W. Midline necrotizing nasal lesions: analysis of 18 cases emphasizing radiological and serological findings with algorithms for diagnosis and management. *Am J Rhinol* 2004; 18:209–219
18. Yang C, Talbot JM, Hwang PH. Bony abnormalities of the paranasal sinuses in patients with Wegener's granulomatosis. *Am J Rhinol* 2001; 15:121–125
19. Aloulah M, Manes RP, Ng YH, et al. Sinonasal manifestations of sarcoidosis: a single institution experience with 38 cases. *Int Forum Allergy Rhinol* 2013; 3:567–572
20. Daum TE, Specks U, Colby TV, et al. Tracheobronchial involvement in Wegener's granulomatosis. *Am J Respir Crit Care Med* 1995; 151:522–526
21. Prince JS, Duhamel DR, Levin DL, Harrell JH, Friedman PJ. Nonneoplastic lesions of the tracheobronchial wall: radiologic findings with bronchoscopic correlation. *RadioGraphics* 2002; 22:S215–S230
22. Polychronopoulos VS, Prakash UB, Golbin JM, Edell ES, Specks U. Airway involvement in Wegener's granulomatosis. *Rheum Dis Clin North Am* 2007; 33:755–775
23. Strange C, Halstead L, Baumann M, Sahn SA. Subglottic stenosis in Wegener's granulomatosis: development during cyclophosphamide treatment with response to carbon dioxide laser therapy. *Thorax* 1990; 45:300–301
24. Marom EM, Goodman PC, McAdams HP. Focal abnormalities of the trachea and main bronchi. *AJR* 2001; 176:707–711
25. Matt BH. Wegener's granulomatosis, acute laryngotracheal airway obstruction and death in a 17-year-old female: case report and review of the literature. *Int J Pediatr Otorhinolaryngol* 1996; 37:163–172
26. Lohrmann C, Uhl M, Kotter E, Burger D, Ghanem N, Langer M. Pulmonary manifestations of Wegener granulomatosis: CT findings in 57 patients and a review of the literature. *Eur J Radiol* 2005; 53:471–477
27. Utz JP, Swensen SJ, Gertz MA. Pulmonary amyloidosis: the Mayo Clinic experience from 1980 to 1993. *Ann Intern Med* 1996; 124:407–413
28. Schmidt J, Pulido JS, Matteson EL. Ocular manifestations of systemic disease: antineutrophil cytoplasmic antibody-associated vasculitis. *Curr Opin Ophthalmol* 2011; 22:489–495
29. Holle JU, Gross WL. Neurological involvement in Wegener's granulomatosis. *Curr Opin Rheumatol* 2011; 23:7–11
30. Fechner FP, Faquin WC, Pilch BZ. Wegener's granulomatosis of the orbit: a clinicopathological study of 15 patients. *Laryngoscope* 2002; 112:1945–1950
31. Montecucco C, Caporali R, Pacchetti C, Turla M. Is Tolosa-Hunt syndrome a limited form of Wegener's granulomatosis? Report of two cases with anti-neutrophil cytoplasmic antibodies. *Br J Rheumatol* 1993; 32:640–641
32. Talar-Williams C, Sneller MC, Langford CA, Smith JA, Cox TA, Robinson MR. Orbital socket contracture: a complication of inflammatory orbital disease in patients with Wegener's granulomatosis. *Br J Ophthalmol* 2005; 89:493–497
33. Mavrikakis I, Rootman J. Diverse clinical presentations of orbital sarcoid. *Am J Ophthalmol* 2007; 144:769–775
34. Weber AL, Jakobiec FA, Sabates NR. Lymphoproliferative disease of the orbit. *Neuroimaging Clin N Am* 1996; 6:93–111
35. Weber AL, Dallow RL, Oot RF. Computed tomography of lymphoproliferative disease of the orbit: report of 50 patients. *Acta Radiol Suppl* 1986; 369:333–336
36. Smoker WR, Gentry LR, Yee NK, Reede DL, Nerad JA. Vascular lesions of the orbit: more than meets the eye. *RadioGraphics* 2008; 28:185–204; quiz, 325
37. Nishino H, Rubino FA, DeRemee RA, Swanson JW, Parisi JE. Neurological involvement in Wegener's granulomatosis: an analysis of 324 consecutive patients at the Mayo Clinic. *Ann Neurol* 1993; 33:4–9
38. Laudien M, Lamprecht P, Hedderich J, Holle J, Ambrosch P. Olfactory dysfunction in Wegener's granulomatosis. *Rhinology* 2009; 47:254–259
39. Haynes BF, Fishman ML, Fauci AS, Wolff SM. The ocular manifestations of Wegener's granulomatosis: fifteen years' experience and review of the literature. *Am J Med* 1977; 63:131–141
40. Foster WP, Greene JS, Millman B. Wegener's granulomatosis presenting as ophthalmoplegia and optic neuropathy. *Otolaryngol Head Neck Surg* 1995; 112:758–762
41. Shah R, Roberson GH, Cure JK. Correlation of MR imaging findings and clinical manifestations in neurosarcoidosis. *AJNR* 2009; 30:953–961
42. Haldorsen IS, Espeland A, Larsson EM. Central nervous system lymphoma: characteristic findings on traditional and advanced imaging. *AJNR* 2011; 32:984–992
43. Keni SP, Wiley EL, Dutra JC, Mellott AL, Barr WG, Altman KW. Skull base Wegener's granulomatosis resulting in multiple cranial neuropathies. *Am J Otolaryngol* 2005; 26:146–149
44. Bradley PJ. Wegener's granulomatosis of the ear. *J Laryngol Otol* 1983; 97:623–626
45. Andrews JT, Kountakis SE. Wegener's granulomatosis of the skull base. *Am J Otolaryngol* 1996; 17:349–352
46. Sharma A, Deshmukh S, Shaikh A, Dabholkar J. Wegener's granulomatosis mimicking skull base osteomyelitis. *J Laryngol Otol* 2012; 126:203–206
47. Murphy JM, Gomez-Anson B, Gillard JH, et al. Wegener granulomatosis: MR imaging findings in brain and meninges. *Radiology* 1999; 213:794–799
48. Choy DS, Weiss A, Lin PT. Progressive multifocal leukoencephalopathy following treatment for Wegener's granulomatosis. *JAMA* 1992; 268:600–601
49. Yong TY, Li JY, Amato L, et al. Pituitary involvement in Wegener's granulomatosis. *Pituitary* 2008; 11:77–84
50. Fujisawa I. Magnetic resonance imaging of the hypothalamic-neurohypophyseal system. *J Neuroendocrinol* 2004; 16:297–302
51. Di Comite G, Bozzolo EP, Praderio L, Tresoldi M, Sabbadini MG. Meningeal involvement in Wegener's granulomatosis is associated with localized disease. *Clin Exp Rheumatol* 2006; 24(suppl 41):S60–S64
52. Sherman JL, Stern BJ. Sarcoidosis of the CNS: comparison of unenhanced and enhanced MR images. *AJR* 1990; 155:1293–1301

(Figures start on next page)

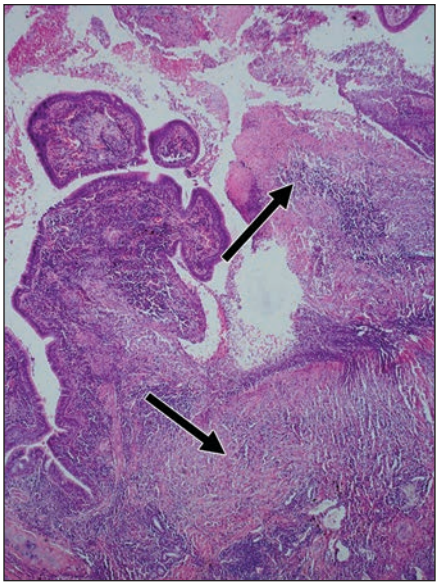

Fig. 1—54-year-old man with granulomatosis with polyangiitis. H and E stain of lung tissue shows necrotizing granulomas (*arrows*).

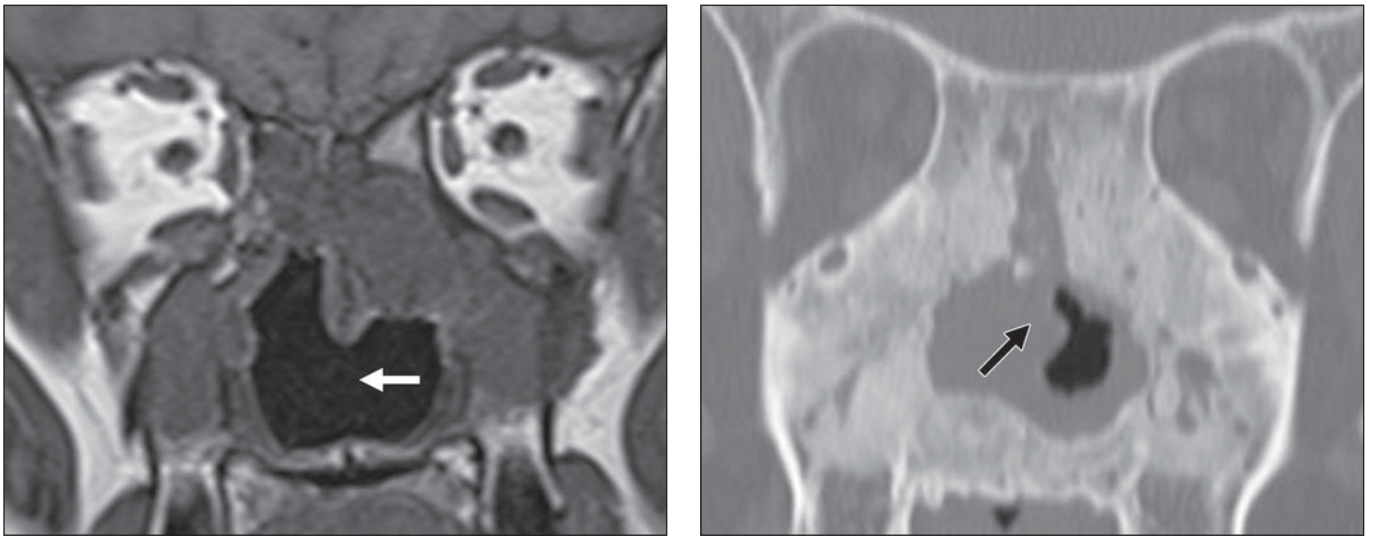

A **B**

Fig. 2—43-year-old woman with granulomatosis with polyangiitis.
A and **B,** Coronal T1-weighted image (**A**) and unenhanced CT image (**B**) show bone destruction with septal perforation (*arrows*). CT image (**B**) shows extensive mucoperiosteal thickening and new bone formation, obliterating sinuses.

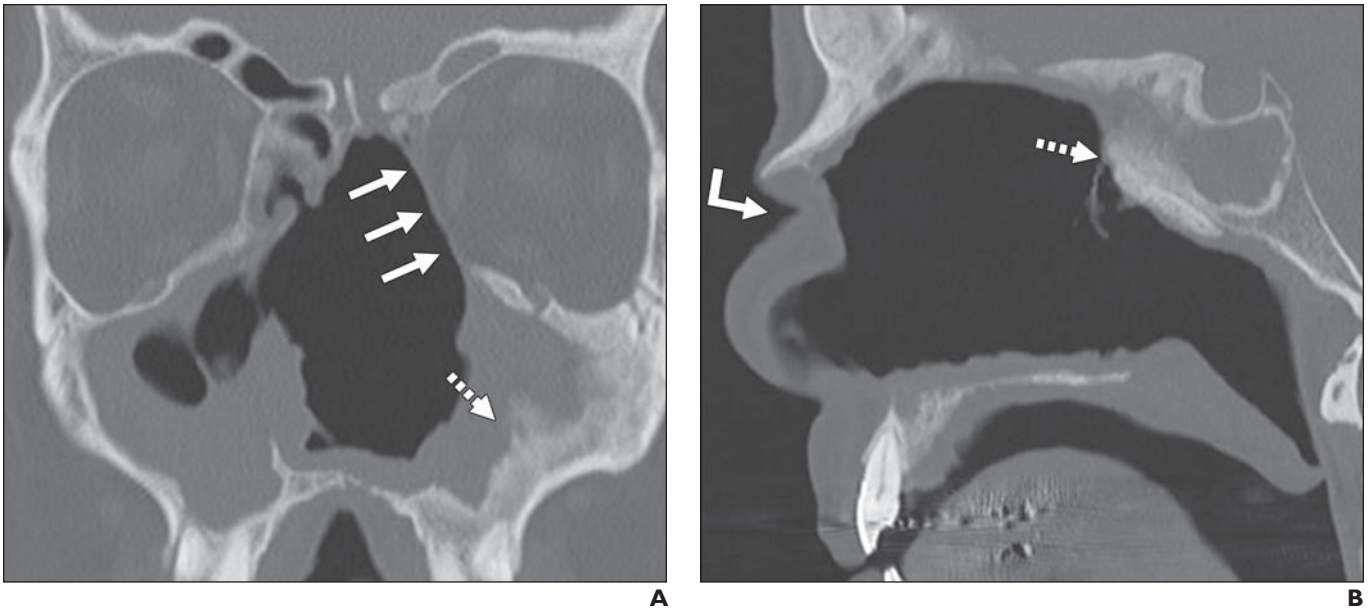

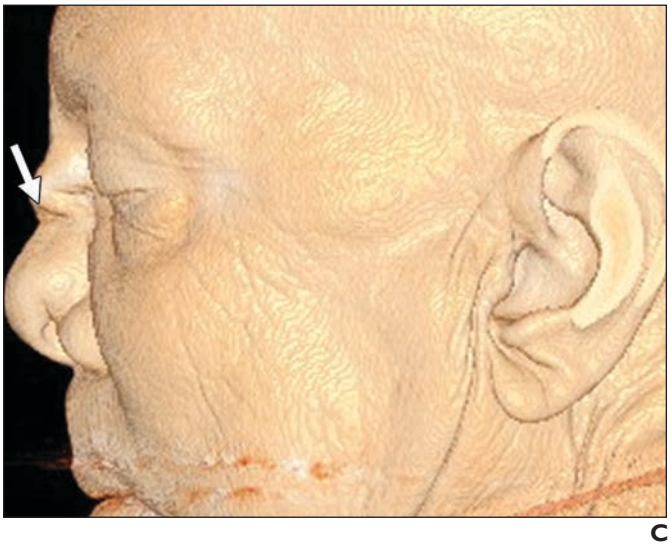

Fig. 3—51-year-old man with granulomatosis with polyangiitis. **A–C,** Coronal (**A**) and sagittal (**B**) unenhanced CT images and 3D reformation (**C**) show extensive midline bone destruction involving lamina papyracea (*solid arrows*, **A**) and new bone formation with leading edge of well-corticated bone (*dashed arrow*, **A** and **B**). Saddlenose deformity is seen (*angled arrow*, **B**; and *arrow*, **C**).

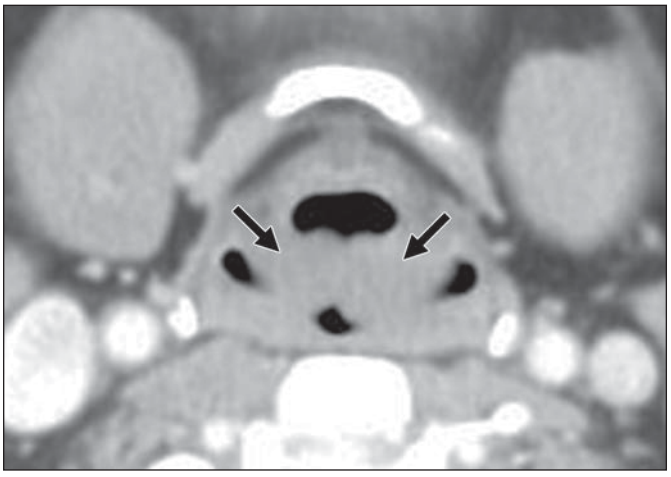

Fig. 4—39-year-old man with granulomatosis with polyangiitis. Axial contrast-enhanced CT image of neck shows masslike soft-tissue infiltration of supraglottic larynx. There is marked thickening of aryepiglottic folds (*arrows*), which appose anterior hypopharyngeal wall.

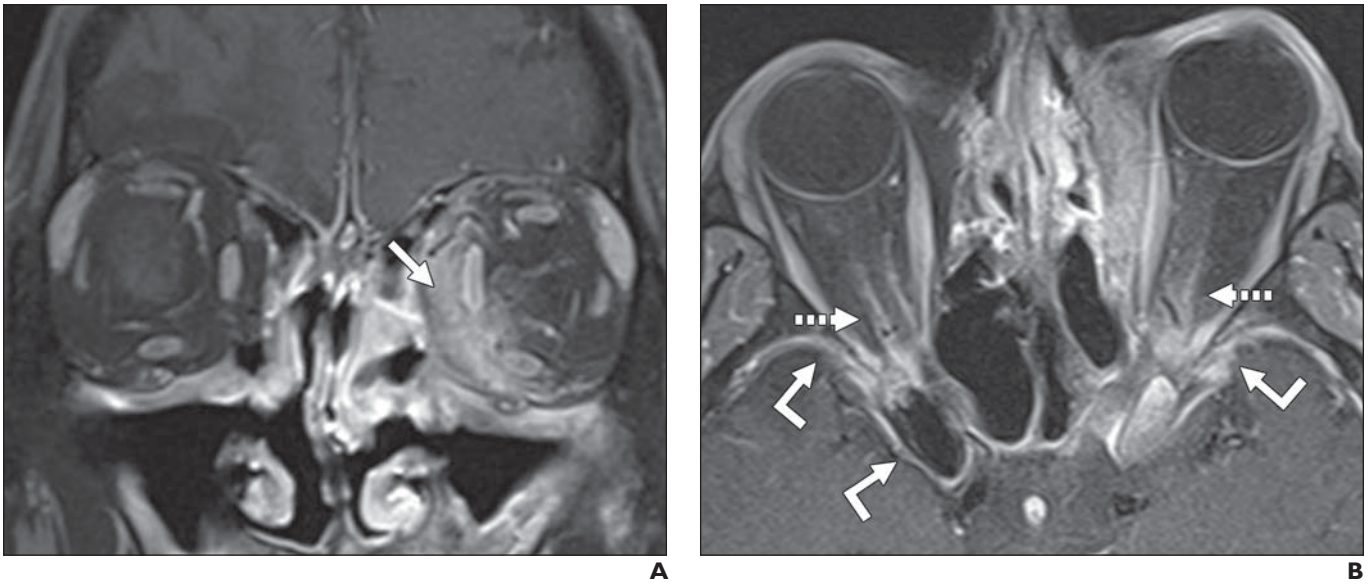

Fig. 5—57-year-old woman with granulomatosis with polyangiitis.
A and **B,** Coronal (**A**) and axial (**B**) contrast-enhanced T1-weighted images show infiltrative enhancing lesion predominantly involving extraconal space (*arrow*, **A**). There is perioptic neuritis (*dashed arrows*, **B**) and pachymeningitis (*angled arrows*, **B**).

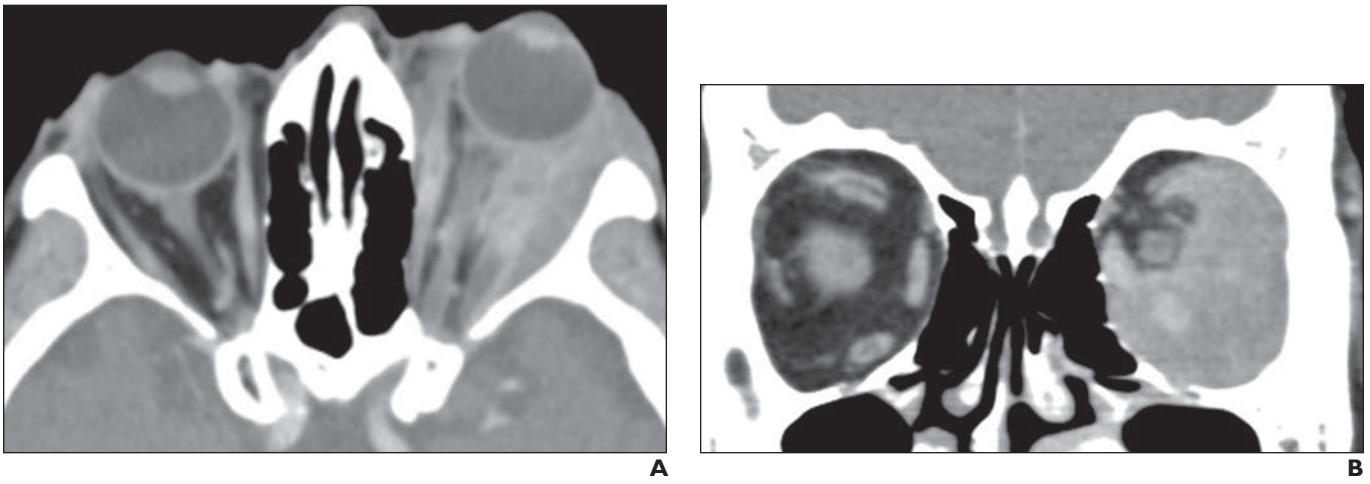

Fig. 6—46-year-old man with granulomatosis with polyangiitis.
A and **B,** Axial (**A**) and coronal (**B**) contrast-enhanced CT images of orbits reveal infiltrative soft-tissue mass involving intra- and extraconal compartments. Note prominent proptosis.

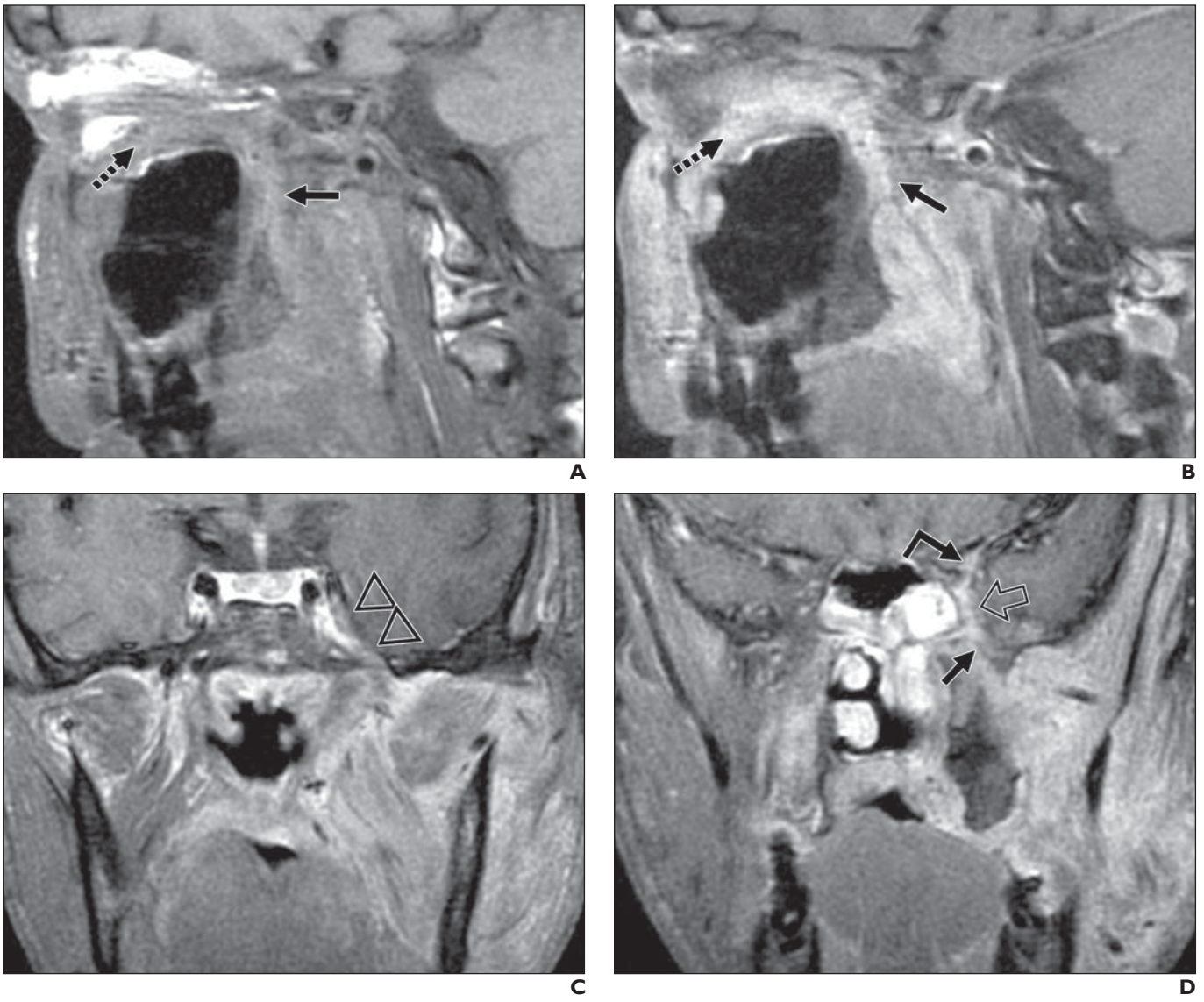

Fig. 7—44-year-old woman with granulomatosis with polyangiitis.
A–D, Sagittal T1-weighted image (**A**), contrast-enhanced T1-weighted image (**B**), coronal contrast-enhanced T1-weighted image (**C**), and coronal T1-weighted image (**D**) show extensive inflammatory changes involving masticator space, orbit (*dashed arrows*, **A** and **B**), and buccal space. Inflammatory changes in masticator space involve muscles of mastication and extend to skull base, with associated thickening and enhancement of third division of trigeminal nerve (*triangles*, **C**). Orbital inflammation extends posteriorly to involve superior (*angled arrow*, **D**) and inferior (*open arrow*, **D**) orbital fissures as well as pterygopalatine fossa (*solid straight arrows*, **A**, **B**, and **D**).

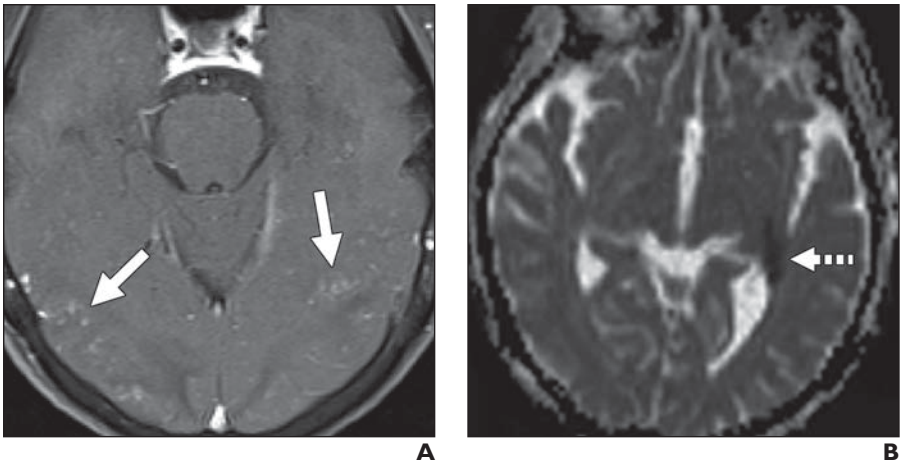

Fig. 8—Two patients with granulomatosis with polyangiitis.
A, 63-year-old man. Axial contrast-enhanced T1-weighted image shows patchy areas of enhancement (*arrows*).
B, 50-year-old man. Axial apparent diffusion–corrected image shows acute infarction in left temporal lobe (*dashed arrow*).

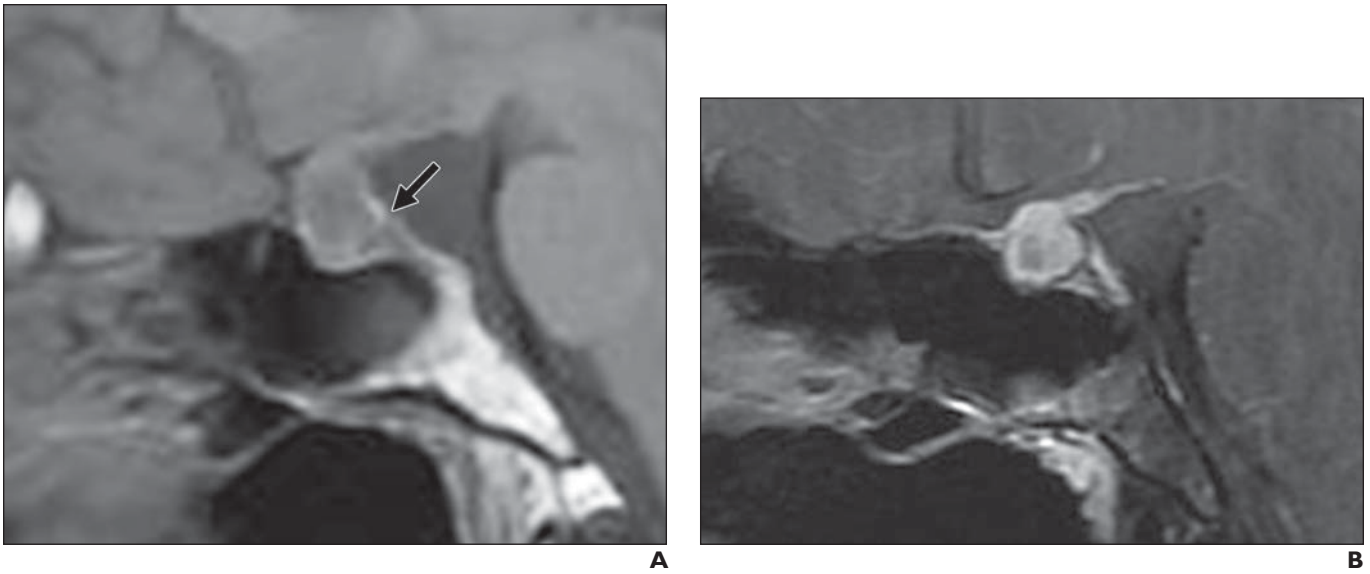

Fig. 9—37-year-old man with granulomatosis with polyangiitis.
A and **B,** Sagittal T1-weighted image (**A**) and contrast-enhanced T1-weighted image (**B**) show pituitary gland enlargement with loss of normal posterior bright spot (*arrow,* **A**) as well as infundibular thickening.

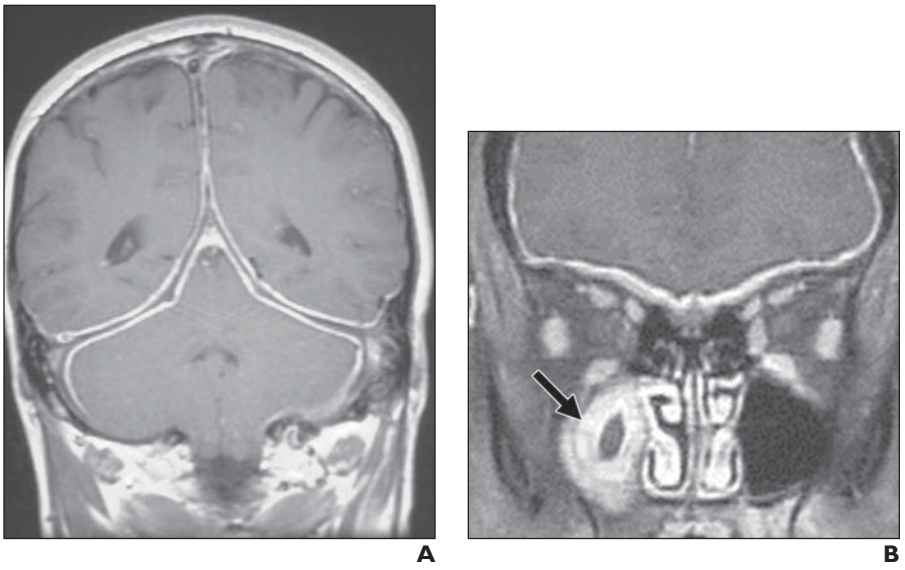

Fig. 10—Two patients with granulomatosis with polyangiitis.
A, 53-year-old man. Coronal contrast-enhanced T1-weighted image shows extensive dural thickening and enhancement.
B, 42-year-old woman. Coronal contrast-enhanced T1-weighted image shows extensive pachymeningeal thickening, most likely resulting from extension of paranasal sinus disease (*arrow*).